Liquid Crystals
Publication details, including instructions for authors and subscription information:
http://www.informaworld.com/smpp/title~content=t713926090

A novel order transition inside the nematic phase of trans -4-hexylcyclohexane-1-carboxylic acid discovered by image processing

B. Montrucchio; A. Sparavigna; S. I. Torgova; A. Strigazzi

Online publication date: 06 August 2010

To cite this Article Montrucchio, B. , Sparavigna, A. , Torgova, S. I. and Strigazzi, A.(1998) 'A novel order transition inside the nematic phase of trans -4-hexylcyclohexane-1-carboxylic acid discovered by image processing', Liquid Crystals, 25: 5, 613 — 620
To link to this Article: DOI: 10.1080/026782998205903
URL: http://dx.doi.org/10.1080/026782998205903

LIQUID CRYSTALS, 1998, VOL. 25, NO. 5, 613–620

A novel order transition inside the nematic phase of *trans*-4-hexylcyclohexane-1-carboxylic acid discovered by image processing

B. MONTRUCCHIO, A. SPARAVIGNA*†§, S. I. TORGOVA‡§
and A. STRIGAZZI†§

Centro Servizi Informatici e Telematici, Politecnico di Torino,
C. Duca degli Abruzzi 24, 10129 Torino, Italy
†Dipartimento di Fisica, and Istituto Nazionale di Fisica della Materia (INFM),
Politecnico di Torino, C. Duca degli Abruzzi 24, 10129 Torino, Italy
‡Organic Intermediates and Dyes Institute, B. Sadovaya 1/4,
103787 Moscow, Russia
§Joint Laboratory on Orientationally Ordered Media (OOM-Lab),
C. Duca degli Abruzzi 24, 10129 Torino, Italy

(*Received 18 May 1998; accepted 29 June 1998*)

We have observed by polarizing microscopy a novel order transition inside the nematic phase and definitely below the clearing point of *trans*-4-hexylcyclohexane-1-carboxylic acid (C_6). The substance is known to exhibit the phase sequence $Cr \rightarrow 32^{\circ}C \rightarrow SmB \rightarrow 47^{\circ}C \rightarrow N \rightarrow 96^{\circ}C \rightarrow I$ (where Cr = crystal, SmB = smectic B, N = nematic, I = isotropic). The order transition, very smooth, was recognized both on cooling and on heating of the sample, consisting of a sandwich cell made by two glass plates unidirectionally rubbed, with a gap around 1 μm. The nematic 'subphase' below the order transition is better ordered (with smaller and more regular domains) than the other 'subphase' above this transition. The data are compared with those obtained for 4-*n*-heptyloxybenzoic acid (HOBA) and already discussed in terms of a surface transition, and are interpreted as due to the presence of smectic cybotactic clusters. To enhance the detection sensitivity, we applied a method of image processing recently introduced by us and also able to reveal soft structural changes in the image frame. Since the method sensitivity is at least 10 times higher with respect to standard techniques, the order transition, even though very smooth (especially on heating), was easily detected, without the necessity for special cell treatment to align the director perfectly in the high temperature nematic phase.

1. Introduction

In the last year, the attention of many researchers in the fields of condensed matter and biological systems has been attracted by substances which exhibit spontaneous twist deformation, even if their molecules are not chiral. A non-chiral lyotropic composition was reported by Usol'tseva *et al.* [1, 2] to exhibit a macroscopic chiral structure, whilst Soto Bustamante *et al.* recently discussed antiferroelectric behaviour in non-chiral thermotropic compounds [3–5]. In these reports, the authors considered the possibility that the effect could be dependent on the behaviour of the hydrogen bonds in the salicylidenamino groups. The hydrogen bonds in such compounds had been shown earlier to be intermolecular [6]. The discovery of spontaneous chiral ordering in the nematic phases of *trans*-4-alkylcyclohexane-1-carboxylic acids (alkyl = butyl and hexyl, here after called C_4 and C_6, respectively) [7], which do not contain any chiral group in the monomeric molecules, renewed interest in the study of these compounds which are mesomorphic due to the formation of cyclic (so-called closed) dimers, via intermolecular hydrogen bonds. The dimer is characterized by a sufficiently elongated shape and by a rigid enough core; if the dimer concentration is greater than a given threshold, the mesophase appears [8]. Among materials forming such dimers, the most well known are two families of organic acids, the first one with a benzene ring in the monomeric molecules and the other with a cyclohexane ring; on both types, extensive studies have been performed [9–12]. To the carboxylic acids with a benzene ring belong two well known acids (4-*n*-heptyloxy- and 4-*n*-octyloxy-benzoic acids, called hereafter HOBA and OOBA, respectively),

*Author for correspondence.

which exhibit smectic C and nematic phases [13–15]; some years ago they were found to show an order transition in the middle of the nematic range [16, 17].

In fact, the existence of a peculiar critical temperature inside the nematic phase of HOBA and OOBA can be simply observed also by means of polarizing microscopy in the orthoscopic mode [18, 19]. On cooling from the isotropic phase, if the surface treatment ensures a well ordered uniform orientation with a certain pretilt in the nematic phase, at a particular critical temperature the uniform alignment changes abruptly into a multidomain structure. On the other hand, on heating from the smectic phase, a softer change occurs over an interval distributed not far from the same temperature, with some hysteresis. But, if in the nematic 'subphase' at higher temperature pretilt is absent, or if the alignment is not sufficiently uniform, on cooling, the order transition is also very soft or even undetectable by usual optical observations.

It is very interesting to look for the existence of a similar order transition in acids like C_4 and C_6, with the aim of understanding the influence of the cyclohexane ring. Furthermore, we wanted to know whether such an order transition is dependent on the existence of a smectic arrangement in the phase sequence of the mesogenic acids (C_4 is reported not to exhibit any smectic phase, whereas C_6 is characterized by a smectic B phase [20, 21]).

To reveal this kind of transition, it was decided to apply the image processing analysis recently introduced by us for detecting soft image changes [22]. This method is particularly useful in conditions where the transition under study is very smooth, implying for instance only a small texture change inside the nematic phase.

In § 2 the experiment is described; in § 3 the application of the image analysis method to the detection of the order transition in C_6 is reported and compared with the case of HOBA, and the conclusions are given in § 4.

2. Experimental

We report here the detection of an order transition in the nematic phase of C_6: it is very clearly revealed, due to the high sensitivity of the image processing technique. On the contrary, such a type of order transition was found to be absent in the nematic phase of C_4. Let us clarify the difference between the two substances: C_4 exhibits no smectic phase, whereas C_6 is characterized by a smectic B phase, from 32°C to 47°C, then becoming nematic up to the clearing point of 96°C [20, 21]. In the case of C_6, the order transition appears at a particular critical temperature of 62°C on heating and shows a big hysteresis on cooling (54°C). The presence of an order transition means that the nematic phase is affected by two different orderings, at low and high temperatures, respectively. They produce two 'subphases' N_1 and N_2, characterized by different textures, with the low temperature 'subphase' N_1 starting on heating from the smectic B–nematic transition. Hence, the relevant optical microscopy is also affected by images having different features.

These results will be compared with those obtained by the optical investigation of the well-known phase- and order-changes of HOBA. HOBA exhibits both smectic C and nematic phases [13, 14], with two 'subphases' N_1 and N_2 in the nematic range; at first glance, the textures in HOBA nematic 'subphases' appear to be similar to those characterizing the C_6 nematic 'subphases'. The presence of the low temperature N_1 'subphase' in HOBA was attributed to the presence of cybotactic clusters having short range smectic C ordering [15].

The experiment here reported involved polarizing microscopic observation in the orthoscopic mode. The cells used were of a common sandwich type, with a gap of 1 μm. The liquid crystal material was introduced by capillarity when it was in the isotropic phase. The inner surfaces of the cell substrates (glass plates) were simply rubbed in order to favour a unidirectional planar alignment in one privileged direction. However, no particular chemical or topographical treatment of the glass plates was used in making up the cells. In this case, the microscopy observations on C_6, made by eye, showed that the transition at the critical temperature T_c between the two nematic 'subphases' was scarcely identifiable on cooling from the isotropic phase, and very difficultly detectable on heating from the smectic phase.

Nevertheless we will show that, following the statistical approach to the data recently developed by us [22], the critical temperature becomes observable without difficulty in both runs, and with a higher sensitivity with respect to simple inspection by eye. This once more demonstrates the power of the proposed method for assisting measurement of soft transition temperatures by means of a proper statistical analysis of the image frame.

The sample was mounted in a Linkam hot stage and the temperature was controlled within 0.1 degree accuracy. The optical investigation was carried out using a Leitz polarizing microscope. A JVC colour CCD camera with fixed shutter was used for recording observations: the digital image acquisition from the camera was made by a colour video digitizer (Play Inc.), driven by a computer. The JVC camera was simultaneously connected to a Grundig S-VHS video recorder and to a Polaroid colour printer.

The transition temperatures observed in the case of C_6 (monomer formula: $C_6H_{13}C_6H_{10}COOH$) are shown in the table and compared with the reference data for

Table. Transition temperatures (°C) for C_6 and HOBA on heating and on cooling: note the hysteresis of almost 5°C. The transition temperature on cooling from the SmB phase to the crystal is below room temperature (*).

On heating	Cr–Sm	Sm–N_1	N_1–N_2	N_2–I
C_6	32	47	62	96
HOBA	90	96	116	142

On Cooling	I–N_2	N_2–N_1	N_1–Sm	Sm–Cr
C_6	91	54	42	*
HOBA	139	113	93	87

HOBA. The latter are in agreement with data reported in last decade by several authors [16–18, 23–26].

In figure 1, typical textures of the smectic B phase (*a*) and of the nematic N_1 (*b*) and N_2 (*c*) 'subphases' are shown for the cyclohexane acid C_6. The smectic phase exhibits a regular 'sandlike' domain structure; the nematic N_1 'subphase' looks quite different from the N_2 'subphase' which shows large areas with a well aligned quasi-planar orientation. In both nematic 'subphases', areas with different birefringence can be observed: in N_1 small domains appear as spots, whereas in N_2 there are large zones with small differences in the light transmitted [12].

Another peculiar feature of C_6 is that on heating, at 92°C—almost 4–5 degrees below the clearing point—the colour of the domains viewed between crossed polarizers abruptly changes, figure 1 (*c*): well oriented red areas with small green domains inside change to a bright green colour and simultaneously the green inclusions change to red; then, after almost two degrees, the domains suddenly return to their original colours. The same colour sequence is again given by the sample on cooling.

In figure 2, typical textures of the smectic C phase (*a*) and of the nematic N_1 (*b*) and N_2 (*c*) 'subphases' are shown for HOBA. Note that the textures of the smectic and the nematic N_1 'subphase' are apparently similar for both C_6 and HOBA; nevertheless, a more refined analysis by means of the above mentioned statistical method reveals substantial differences.

3. Analysis method and discussion

In principle, several standard methods can be used for analysing and classifying images and for defining the statistical distances between them. In any case, the texture discrimination can be done by choosing a set

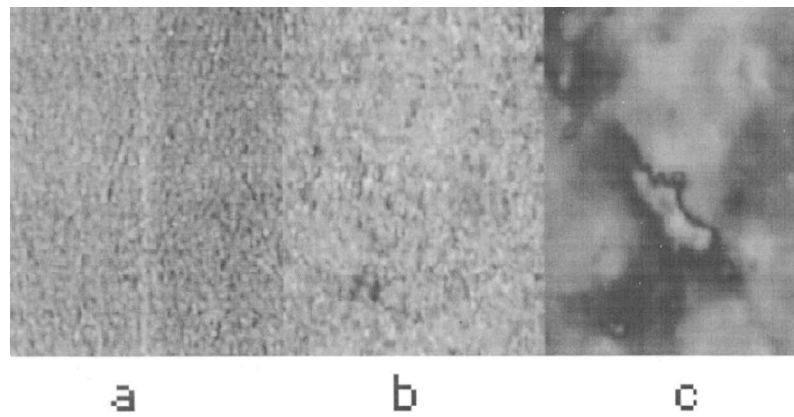

Figure 1. Textures of *trans*-4-hexylcyclohexane-1-carboxylic acid (C_6) in the smectic B phase at 44°C (*a*) and in the two nematic 'subphases' at low (*b*) and high (*c*) temperature, 54°C and 90°C, respectively (note that the order transition was found to occur at 62°C). The image of the high temperature nematic phase (*c*) consists of several almost uniform areas of bright green colour, with a small red region in the middle. The size of each figure is $340 \times 500\,\mu m^2$.

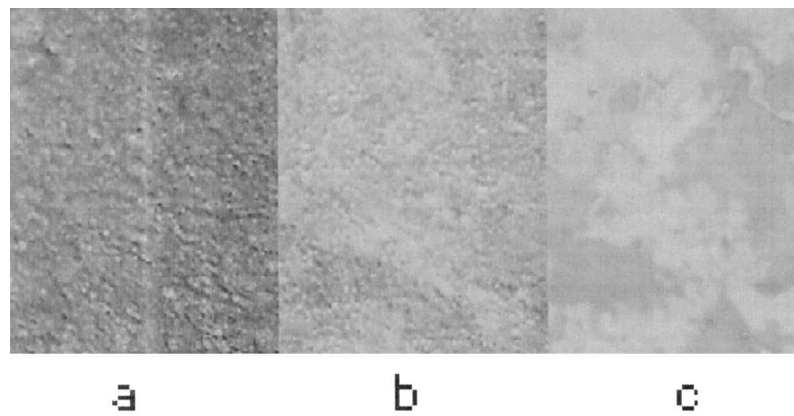

Figure 2. Textures of 4-*n*-heptyloxybenzoic acid (HOBA) in the smectic C phase at 92°C (*a*) and in the two nematic 'subphases' at low (*b*) and high (*c*) temperature, 110°C and 130°C, respectively (the critical temperature between the two nematic 'subphases' was found to be 116°C on heating). The image of the high temperature nematic phase (*c*) consists of several almost uniform areas. The size of each figure is $340 \times 500\,\mu m^2$.

of parameters which account for the main spatial organization of the image, whereas the model underlying the parameters can be either structural or statistical [27–30].

The application of the image statistical treatment to the optical investigation of liquid crystals textures is very important in enhancing the detection sensitivity, which allows an easier texture recognition. In a recent paper [22], we proposed and described a statistical approach to the detection of smooth image changes. Here we limit ourselves to a brief summary of such a processing method, pointing out its features.

In the image recorded by the microscope camera, we consider as position and dispersion indices, the mean intensity of the transmitted light, averaged over the whole window (which can be the entire beam cross section or a certain part of it) and the kth order moments of the light intensity distribution (where $k = 1, n$ with n defined *a priori*) [31–33]. Of course, the mean intensity can be defined as the $k = 0$th order moment. All these parameters are extremely sensitive to the texture changes of the liquid crystal sample, and thus can be very useful for the investigation of any structure change caused by either order- or phase-transitions of the material.

Actually, the moments description cannot follow the local spatial character of the image frame, since this particular information is hidden in the averaging procedure. Moreover, we remind the reader that it is necessary to distinguish between image- and object-characters: for instance, a privileged direction in the object can correspond to the absence of any privileged directions in the image (a uniformly planar aligned cell gives a uniform black image using crossed polarizers); on the other hand, a texture change in the image can be due simply to a rotation of the same unchanged object between crossed polarizers. Nevertheless, a characterization can be easily performed on the image frame concerning the image anisotropy and coarseness to be attributed essentially to sample features, i.e. to the smectic or to the nematic phase of the mesomorphic compounds [22].

Through the signal coming from the video digitizer, the true colour image detected by the CCD camera is stored in a file with a resolution of 640×480 squared pixels. The file is elaborated on a Digital Alpha Workstation DEC255 by original C-software prepared by the authors. Such a program is able to scan and to analyse the image frame, choosing one of the three fundamental colours (red, green and blue). In our case we chose the green and the red for the C_6 analysis and the green (the most sensitive) for HOBA, since this latter material does not show any particular colour change in the heating scan: in this case the results would be quite similar, simply translating the whole RGB image into a unique integrated grey scale.

To each pixel at the arbitrary point $P(x, y)$ in the image frame our C-program associates a colour tone b (red or green) ranging from 0 to 255: $b(x, y)$ is then a 2-dimensional function representative of the image intensity (brightness) distribution over the whole image frame.

Starting from the function $b(x, y)$, which gives the pixel colour tone, the following calculations can be performed. First, the mean intensity of the colour tone is calculated:

$$\mathcal{M}_0 = \frac{1}{l_x l_y} \int_0^{l_x} \int_0^{l_y} b(x, y)\, \mathrm{d}x\, \mathrm{d}y \tag{1}$$

where l_x, l_y are the x and y rectangular range of the image frame.

k rank statistical moments of the image can also be defined in the following way:

$$\mathcal{M}_k = \frac{1}{l_x l_y} \int_0^{l_z} \int_0^{l_y} [b(x, y) - \mathcal{M}_0]^k\, \mathrm{d}x\, \mathrm{d}y. \tag{2}$$

All integrals can be calculated for the whole image or a window identifying an object. In the latter case, the moments $\mathcal{M}_0$ and $\mathcal{M}_k$ allow the determination of the position and the mean shape of the object. These concepts are very useful in a microscopic investigation for the detection of defects and for the recognition of non-homogeneous structures [32, 33].

Since at first glance the images relevant to the nematic N_1 and the smectic phases (see figure 1) look more or less homogeneous, we use the moments $\mathcal{M}_0$ and $\mathcal{M}_k$ defined by equations (1, 2) for the whole image, supposing it to be characterized by only one statistical distribution of the intensity. *A posteriori*, such a hypothesis of homogeneity was justified.

For checking the hypotheses of homogeneity and isotropy of the image frame, we proposed a set of local and integrated coherence lengths [22], defined in the following way. Starting from an arbitrary point $P(x, y)$ of the figure $b(x, y)$, we calculated along the eight radial directions taken at 45 degrees from each other the average directional moments $\mathcal{M}_0^i(x, y)$, $\mathcal{M}_k^i(x, y)$:

$$\mathcal{M}_0^i(x, y) = \frac{1}{l_{0i}} \int_0^{l_{0i}} b(x + r \sin\theta_i, y + r \cos\theta_i)\, \mathrm{d}r \tag{3}$$

$$\mathcal{M}_k^i(x, y) = \frac{1}{l_{ki}} \int_0^{l_{ki}} [b(x + r \sin\theta_i, y + r \cos\theta_i) - \mathcal{M}_0^i(x, y)]^k\, \mathrm{d}r \tag{4}$$

where the index i ranges over all directions from 1 to 8, r is the radial distance from P, and θ_i is the angle formed by the i-direction with the y-axis. The lengths l_{0i} and l_{ki}

are defined as the radial distances (from P) at which the values of the directional moments $\mathcal{M}_0^i(x, y)$ and $\mathcal{M}_k^i(x, y)$ saturate, within a confidence level τ, to the moments of the same rank $\mathcal{M}_0$ and $\mathcal{M}_k$, averaged over the entire image frame. In this way the local coherence lengths $l_{0i}(x, y)$ and $l_{ki}(x, y)$ are defined. Note that the moments $\mathcal{M}_0^i(x, y)$, $\mathcal{M}_k^i(x, y)$ are not calculated over a window as a surface, but along eight directions. Thus our method is different from the standard statistical approach, allowing us to take naturally into account, together with the homogeneity, the image anisotropy which is very important in the problem of texture recognition.

At this point, it is possible to integrate, introducing the mean values of the previous coherence lengths averaged over the whole window:

$$L_{0i} = \frac{1}{l_x l_y} \int_0^{l_x} \int_0^{l_y} l_{0i}(x, y)\, \mathrm{d}x\, \mathrm{d}y \qquad (5)$$

$$L_{ki} = \frac{1}{l_x l_y} \int_0^{l_x} \int_0^{l_y} l_{ki}(x, y)\, \mathrm{d}x\, \mathrm{d}y. \qquad (6)$$

We used such averaged lengths to define the coarseness of the texture in the plane (x, y) for the smectic and the nematic N_1, N_2 'subphases', applying our method of image analysis to the high sensitivity detection of the phase- and order-transitions in C_6; as compared with HOBA.

After collecting a set of image frames of the liquid crystal cell scanned at different temperatures, by imposing a controlled temperature rate (1 degree min^{-1}) during heating and cooling in the range (room temperature–clearing point) of the material under study, the histogram of the occurrence number $\mathcal{N}$ of the colour tone b was calculated for each image frame.

In figure 3, the brightness occurrence of red (upper part) and green (lower part) during the temperature scanning of C_6 (on heating) is presented (the images reported in figure 1 were taken during such a scanning). Here the colour tone b varies along the vertical axis, and its occurrence number $\mathcal{N}$ is translated into a convenient grey tone.

One can immediately recognize the transition from smectic B to nematic N_1, the 'subphase' order transition $N_1 \rightarrow N_2$ and the clearing point. Let us stress that by using our analysis method all the transitions are detectable with high sensitivity; in particular, the critical point $N_1 \rightarrow N_2$ (the order transition) too becomes clearly detectable, even in the case when it is very smooth by eye inspection.

In figure 4, the mean intensity- and the variance-curves of the histograms shown in figure 3 are recorded by the thick and thin lines, respectively: the curves

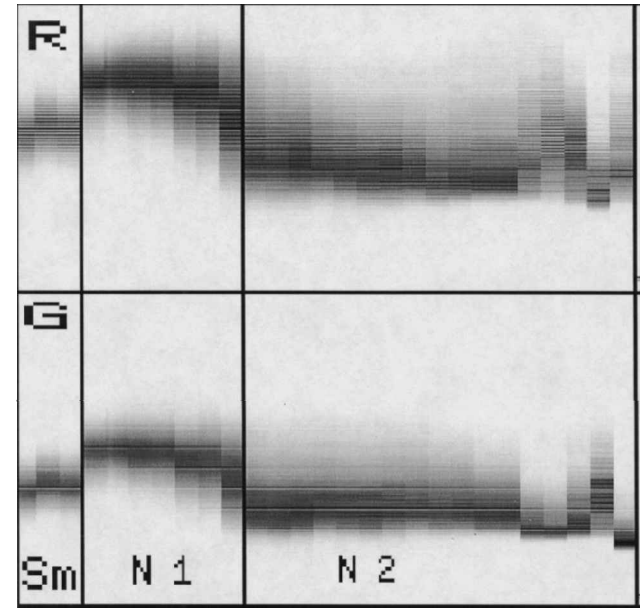

Figure 3. Brightness occurrence of the colour under consideration over the entire image frame during a temperature scan (on heating) for C_6. The upper and the lower parts of the figure show the red and the green colour tone b of the same image, respectively. The tone scale varies along the vertical axis and the colour tone occurrence number $\mathcal{N}$ is translated into a grey tone. Black indicates the highest occurrence of that tone; white indicates no occurrence. The temperature varies along the horizontal axis and the image mapping was chosen with a step interval of two degrees. The figure therefore shows the dynamics of the occurrence dispersion during the temperature scan giving evidence of the phase and order transitions. Such transitions are at 47°C for $SmB \rightarrow N_1$, 62°C for $N_1 \rightarrow N_2$ and the clearing point is at 96°C.

representing the variance clearly show, besides the phase transitions, the textural transition from the optically scattering 'subphase' (N_1) to the more uniform subphase (N_2). The curve relevant to the mean intensity highlights the phase transitions and the textural transition, since both the intensity and dispersion of the transmitted light change in the phase and in the 'subphase' transitions.

Let us stress that the present method of investigating the optical behaviour of the liquid crystal cell allows the detection of the textural order transitions between the two 'subphases' with a sensitivity comparable to that for the detection of the transitions from crystal to smectic, from smectic to nematic and from nematic to isotropic phases.

In figure 5 the mean intensity and variance for a temperature scan on HOBA are shown for comparison. In this case, the curve reporting the mean intensity highlights the phase much more than the order transition, due to the fact that the transmitted light is almost equal in the two 'subphases'; it is now only the

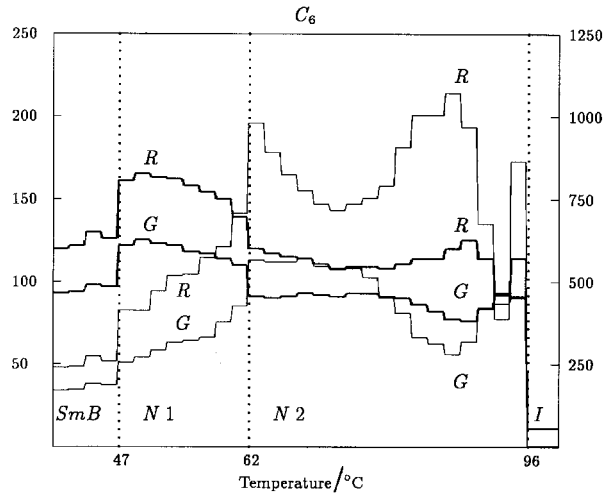

Figure 4. Temperature dependence, on heating, of the mean intensity (thick line) and of the variance (thin line) of the transmitted light for the red and green tone $b(x, y)$ of the images, in the case of the C_6 sample. The y-scales are related to the colour tone units—the left scale, arbitrary (from 0 to 255) refers to the intensity, the right scale (unit squared with respect to the previous one), refers to the variance. Note the order transition between the N_1 and N_2 'subphases' at 62°C, clearly evidenced by both intensity- and variance-curves. Notice also the colour change at about four degrees below the clearing point.

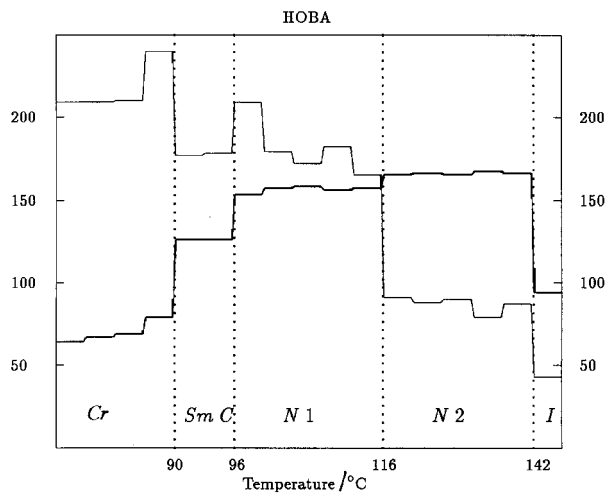

Figure 5. Temperature dependence, on heating, of the mean intensity (thick line) and of the variance (thin line) of the transmitted light for the green tone $b(x, y)$ of the images, in the case of HOBA. The y-scales are related to the colour tone units—the left scale, arbitrary (from 0 to 255) refers to the intensity, the right scale (unit squared with respect to the previous one), refers to the variance. This figure is reported for comparison of the behaviour of HOBA with that of C_6 (see figure 4). Note that here the order transition between the N_1 and N_2 'subphases' appears at 116°C, and is clearly evidenced by the variance- and not by the intensity-curve.

variance behaviour which reveals the presence of the two different 'subphases'.

By comparing the change of the variance at the order transition with the corresponding intensity change, we realize that the moments statistics method can be at least ten times more sensitive than standard methods based only on the detection of the transmitted light intensity.

An analysis of the coarseness of the images has also been performed, with the aim of determining whether the smectic texture is always characterized by a different size of the grains with respect to the low temperature nematic 'subphase' N_1. It is interesting to compare the previous textures with the texture corresponding to the nematic 'subphase' N_2, which exhibits practically no grains, but a schlieren structure, and to determine what the relative sizes of the domains are in the two nematic 'subphases'. Thus we calculated the mean values of the previously introduced coherence lengths L_{0i}, from equation (5), along the eight i-directions, each at 45 degrees, scanning with the position of the starting point the entire window of the image frame. In fact, if we compare two image frames, one with the intensity described by a gaussian, and the other made by small quasi-regular domains (like a chessboard), a coherence length defined as in the first case practically coincides with the double standard deviation; in the second case, it is given by the double grain size taken in the same direction, then decreasing with the sample coarseness. Moreover, the coherence length turns out to be contrast-independent, as one can realize when considering two chessboards with the same pitch, but one with high contrast black–white, and the other with a low contrast sinusoidal grey scale. As a conclusion, the image frames exhibit a coherence length proportional to the average grain size.

The figures of merit of the texture coarseness in the plane (x, y) for the smectic and the nematic N_1, N_2 'subphases' in the case of C_6 are shown in figure 6(*a*), in comparison with the same figure of merit already found in the case of HOBA, figure 6(*b*). In both cases the confidence level was conventionally established at 5%, and the colour tone analysed was green for both materials. By converting images to the integrated grey scale, no significant variations in the figures of merit were found.

Although at first glance the corresponding textures of C_6 shown in figure 1 and those of HOBA reported in figure 2 look more or less similar; nevertheless the coarseness figure of merit reveals a substantially different behaviour of the grain size with temperature. In fact, the C_6 and HOBA images (*a*), relevant to the smectic phase, exhibit practically the same grain size (10–15 μm), somewhat elongated in one direction, and the figure of merit

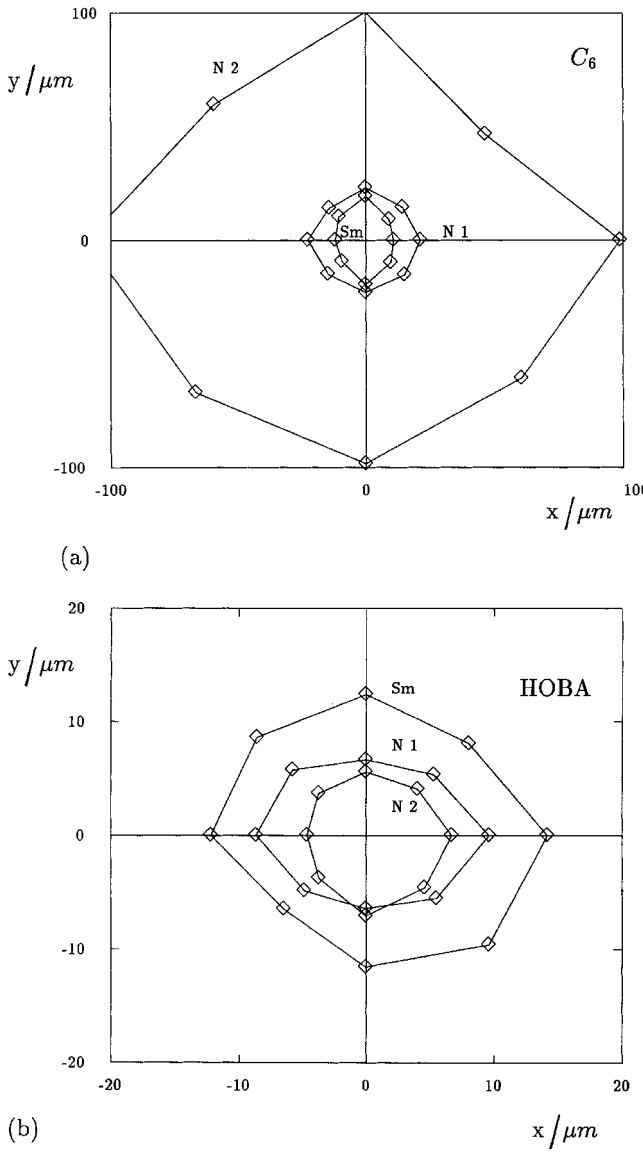

Figure 6. Figure of merit providing the mean coherence lengths L_{0i} for the smectic and the two nematic 'subphases:': (*a*) for the images relevant to C_6, shown in figure 1, and (*b*) for the images relevant to HOBA, reported in figure 2. The radial distance defining the figure of merit is practically coincident with the average domain size taken in that direction: then the figures of merit estimate the directional coarseness of the texture in the smectic phase and in the 'subphase' N_1; however, in the nematic N_2 'subphase', the figure of merit gives the double standard deviation of the distribution. The grain size for both materials is practically the same in the smectic phase, whereas it is different in the N_1 'subphase'. Let us note also that the figure of merit of the N_2 'subphase' in HOBA is the smaller one, since the 'subphase' is characterized by a much more uniform schlieren texture, resulting in a diminishing of the intensity standard deviation, see figure 2 (*c*).

has the same elliptical shape and the same area (with the accidental exchange x–y in the image). But, on increasing the temperature, when crossing the smectic–nematic transition, the C_6 image enlarges the grain size a little, see figure 1 (*a, b*): then the N_1 figure of merit has a greater area than the SmB figure of merit. Later, at the order transition point, the resulting schlieren texture of the image, figure 1 (*c*), produces a figure of merit for N_2 comparable to the double standard deviation of the distribution.

On the other hand, on heating through the smectic–nematic transition, the HOBA image moved towards a situation with a slightly smaller grain size, figure 2 (*a, b*), and then the N_1 figure of merit is a subset of the SmC figure of merit. Moreover, on crossing the order transition point, the N_2 'subphase' was characterized by a much more uniform schlieren texture, resulting in a diminishing of the intensity standard deviation, see figure 2 (*c*). Thus the relevant figure of merit is included in the previous one.

The presence in HOBA of a nematic low temperature 'subphase', more ordered than the usual nematic phase (also from a microscopic point of view), was explained as being due to the presence of a short range smectic C ordering above the smectic–nematic transition (pre-transitional cybotactic clusters [15, 19, 23]). We can explain the analogous texture in C_6 as being due to the occurrence of smectic B ordering, also providing cybotactic clusters.

4. Conclusions

We have investigated by polarizing microscopy the textures of thin layers of two homologous *trans*-4-alkylcyclohexane-1-carboxylic acids (alkyl = butyl, C_4, and = hexyl, C_6). These substances are mesogens since they form intermolecular H-bonds; they are known to exhibit the phase sequence $Cr \rightarrow 36°C \rightarrow N \rightarrow 86°C \rightarrow I$, and $Cr \rightarrow 32°C \rightarrow SmB \rightarrow 47°C \rightarrow N \rightarrow 96°C \rightarrow I$, respectively. We have found a novel order transition inside the nematic phase only in C_6, the substance which is characterized by a smectic B phase. The order transition, very smooth, was recognized both on cooling and on heating. The nematic 'subphase' below the order transition was found to be better ordered (with smaller and more regular domains) than the other 'subphase' above the same transition. There was no necessity for a special treatment of the cell plates to align the director in the high temperature nematic phase, since we applied a method of image processing recently introduced by us that is able to reveal soft structural changes in the image frame. The sensitivity of the method is at least 10 times higher with respect to standard techniques. The data, compared with the results previously obtained for HOBA, are interpreted as being due to the presence of

smectic cybotactic clusters which appear only in the low temperature part of the nematic range in C_6.

One of us (SIT) acknowledges the support of the Politecnico di Torino in the frame of the Agreement with the Russian Academy of Sciences.

References

[1] Usol'tseva, N., Praefcke, K., and Blunk, D., 1997, European Conference on Liquid Crystals, ECLC'97, Zakopane, 3–8 March, O-60, p. 85, *SPIE Proc*., **3319,** 319.

[2] Blunk, D., Praefcke, K., and Usol'tseva, N., 1997, A novel case of spontaneous formation of chirality: observation in lyotropic compositions of a non-chiral disc-like material in alkanes, Workshop Sfb 335 'Anisotrope Fluide', Technical University, Berlin, December 10–11, 1997.

[3] Soto Bustamante, E. A., Yablonsky, S. V., Ostrovskii, B. I., Beresnev, L. A., Blinov, L. M., Haase, W., and Garay, L., 1997, in Abstracts of III CIAFC, Pucon, December 1–5, 1997, p. 22.

[4] Soto Bustamante, E. A., Yablonsky, S. V., Ostrovskii, B. I., Beresnev, L. A., Blinov, L. M., and Haase, W., 1998, *Liq. Cryst*. (in the press).

[5] Soto Bustamante, E. A., Yablonsky, S. V., Ostrovskii, B. I., Beresnev, L. A., Blinov, L. M., and Haase, W., 1997, Antiferroelectric behaviour of achiral mesogenic polymer mixtures, Workshop Sfb 335 'Anisotrope Fluide', Technical University, Berlin, December 10–11, 1997.

[6] Bolotin, B. M., Lazareva, V. T., Titov, V. V., and Torgova, S. I., 1976, in Proceedings of Conference on Liquid Crystals and their Practical Applications, Ivanovo, 1976, p. 130–135.

[7] Torgova, S. I., Komitov, L., and Strigazzi, A., 1998, *Liq. Cryst*., **24,** 131.

[8] Torgova, S. I., Abramic, D., Strigazzi, A., and Zumer, S., 1998, European Conference on Liquid Crystals, ECLC'97, Zakopane, 3–8 March, 1997, A-3, p. 105, *SPIE Proc*., **3319,** 201.

[9] Gray, G. W., Jones, B., and Marson, F., 1957, *J. chem. Soc*., **53,** 393.

[10] Gray, G. W., and Winsor, P. A., 1974, *Mol. Cryst. liq. Cryst*., **26,** 305.

[11] Gray, G. W., and McDonnell, D. G., 1978, *Mol. Cryst. liq. Cryst*., **53,** 147.

[12] Coates, D., and Gray, G. W., 1976, *The Microscope*, **24,** 117.

[13] Gray, G. W., and Jones, B., 1953, *J. chem. Soc*., **41,** 79.

[14] Herbert, A. J., 1967, *Trans. Faraday. Soc*., **63,** 555.

[15] DeVries, A., 1970, *Mol. Cryst. liq. Cryst*., **10,** 31.

[16] Simova, P., and Petrov, M., 1983, *Phys. Status Solidi A*, **80,** K153.

[17] Petrov, M., and Simova, P., 1985, *J. Phys. D: appl. Phys*., **18,** 239.

[18] Petrov, M., Braslau, A., Levelut, A. M., and Durand, G., 1992, *J. Phys. II (Fr.)*, **2,** 1159.

[19] Barbero, G., Komitov, L., Petrov, M., and Strigazzi, A., 1991, *Int. J. mod. Phys. B*, **5,** 2229.

[20] Molochko, V. A., Ivashchenko, A. V., Lidin, P. A., and Torgova, S. I., 1989, *Zh. Priclodnoi Chimii*, **62,** 1605.

[21] Molochko, V. A., Ivashchenko, A. V., Lidin, P. A., and Torgova, S. I., 1990, *J. Appl. Chem*., **62,** 1486.

[22] Montrucchio, B., Sparavigna, A., and Strigazzi, A., 1998, *Liq. Cryst*., **24,** 841, downloadable by: http://www.polito.it/~amelia/LIQCRYST/Image.ps.gz

[23] Frunza, L., Frunza, S., Petrov, M., Sparavigna, A., and Torgova, S. I., 1996, *Mol. Mater*., **6,** 215.

[24] Bryan, R. F., Hartley, P., Miller, R. W., and Ming-Shing, S., 1980, *Mol. Cryst. liq. Cryst*., **62,** 281.

[25] Neubert, M. E., and De Vries, A., 1987, *Mol. Cryst. liq. Cryst*., **145,** 1.

[26] Petrov, M., Anachkova, E., Kirova, N., Ratajczak, H., and Baran, J., 1994, *J. mol. Liq*., **62,** 221.

[27] Haralick, R. M., 1979, *Proc. IEEE*, **67,** 786.

[28] Weszka, J. S., Dyer, C. R., and Rosenfeld, A., 1976, *IEEE Trans. Syst., man., Cybern*., **6,** 369.

[29] Azencott, R., Wang, J., and Younes, L., 1997, *IEEE Trans., Pattern Analysis and Machine Intelligence*, **19,** 148.

[30] Haralick, R. M., Shanmugan, K., and Dinstein, I., 1973, *IEEE Trans. Syst., man., Cybern*., **3,** 610.

[31] Pitas, I., 1993, *Digital Image Processing Algorithms* (Cambridge: Prentice Hall).

[32] Jähne, B., 1993, *Digital Image Processing* (Berlin: Springer Verlag).

[33] Teuber, J., 1993, *Digital Image Processing* (New York: Prentice Hall).